ANNALS of Clinical and Translational Neurology
Open Access
ANA American Neurological Association since 1875

RESEARCH ARTICLE

αCAR IGF-1 vector targeting of motor neurons ameliorates disease progression in ALS mice

Ioanna Eleftheriadou[1], Ioannis Manolaras[1], Elaine E. Irvine[2], Michael Dieringer[1], Antonio Trabalza[1] & Nicholas D. Mazarakis[1]

[1]Gene Therapy, Centre for Neuroinflammation & Neurodegeneration, Division of Brain Sciences, Faculty of Medicine, Imperial College London, Hammersmith Hospital Campus, London W12 0NN, UK
[2]Metabolic Signaling Group, MRC Clinical Sciences Centre, Imperial College London, Hammersmith Hospital Campus, London W12 0NN, UK

Correspondence
Nicholas D. Mazarakis, Gene Therapy, Centre for Neuroinflammation & Neurodegeneration, Division of Brain Sciences, Faculty of Medicine, Imperial College London, Hammersmith Hospital Campus, London W12 0NN, UK. Tel: +44(0)2075947024; Fax: +44(0)2075943200; E-mail: n.mazarakis@imperial.ac.uk

Funding Information
This work was supported by a Seventh Framework Programme European Research Council Advanced Grant, no: 233147 and a Proof of Concept Grant no: 620253 to N.D.M. supporting I.E.

Received: 14 April 2016; Revised: 13 June 2016; Accepted: 28 June 2016

Annals of Clinical and Translational Neurology **2016; 3(10): 752–768**

doi: 10.1002/acn3.335

Abstract

Objective: We have previously described the generation of coxsackievirus and adenovirus receptor (αCAR)-targeted vector, and shown that intramuscular delivery in mouse leg muscles resulted in specific retrograde transduction of lumbar-motor neurons (MNs). Here, we utilized the αCAR-targeted vector to investigate the in vivo neuroprotective effects of lentivirally expressed *IGF-1* for inducing neuronal survival and ameliorating the neuropathology and behavioral phenotypes of the $SOD1^{G93A}$ mouse model of ALS. **Methods**: We produced cell factories of *IGF-1* expressing lentiviral vectors (LVs) bearing αCAR or Vesicular Stomatitis Virus glycoprotein (VSV-G) on their surface so as to compare neuroprotection from MN transduced versus muscle transduced cells. We performed intramuscular delivery of either αCAR *IGF-1* or VSVG *IGF-1* LVs into key muscles of $SOD1^{G93A}$ mice prior to disease onset at day 28. Motor performance, coordination and gait analysis were assessed weekly. **Results**: We observed substantial therapeutic efficacy only with the αCAR *IGF-1* LV pretreatment with up to 50% extension of survival compared to controls. αCAR *IGF-1* LV-treated animals retained muscle tone and had better motor performance during their prolonged survival. Histological analysis of spinal cord samples at end-stage further confirmed that αCAR *IGF-1* LV treatment delays disease onset by increasing MN survival compared with age-matched controls. Intrastriatal injection of αCAR *eGFP* LV in rats leads to transduction of neurons and glia locally and neurons in olfactory bulb distally. **Interpretation**: Our data are indicative of the efficacy of the αCAR *IGF-1* LV in this model and support its candidacy for early noninvasive neuroprotective therapy in ALS.

Introduction

Amyotrophic lateral sclerosis (ALS) is a devastating adult-onset progressive neurodegenerative disorder, characterized by the combined degeneration of upper and lower motor neurons that reside in the spinal cord, brain stem, and cortex. Affected individuals die 2–5 years following diagnosis.[1] ALS cases are mainly sporadic (SALS) and only 10% exhibit an autosomal dominant mode of inheritance (familial ALS or FALS).[2] One-fifth of FALS cases are caused by mutations in the Cu/Zn superoxide dismutase-1 (SOD1) gene.[3] Transgenic mice that overexpress the mutant human SOD1 protein (various mutants with G93A being the most aggressive) have been derived and predominantly used as models of disease. These mice develop a severe and progressive motor impairment leading to hind limb paralysis resembling ALS pathology in humans.[4]

The *IGF-1* family of growth factors (somatomedins) includes three structurally related ligands (*IGF-1*, *IGF-2* and insulin), their respective receptors, and at least six *IGF-1* binding proteins (*IGFBP*).[5] They are produced in multiple cells and exert different physiological roles by binding to distinct tyrosine kinase receptors and activating multiple downstream signaling cascades.[6] Insulin-like growth factor 1 (*IGF-1* or somatomedin C) has been shown to interact with *IGF-1R* and can induce pleiotropic effects, including neuroprotective ones, by inhibiting

apoptosis.[7] The majority of circulating *IGF-1* is bound and sequestered by *IGFBPs*, thus extending its half-life, and controlling its distribution/bioavailability in various tissues.

Gene delivery of neurotrophic molecules, including *IGF-1*, shown to have a therapeutic effect on MN survival, could be a possible gene therapy strategy for ALS.[8,9] In recent years, many studies have focused on gene delivery of growth factors to the central nervous system (CNS) in order to slow disease progression in animal models of ALS utilizing the intramuscular,[10–13] intracerebral,[14,15] intracerebroventricular[16], and intraspinal[17,18] routes of administration. Despite the encouraging results of these studies, subcutaneous delivery of recombinant human insulin-like growth factor 1 IGF-1 (*rhIGF-1)* in ALS patients had little effect in 3 clinical trials.[19–21] Each of these approaches has its own limitations which may negate achieving efficacy in ALS patients. Thus, it is clear that there is an urgent need to develop new therapeutic strategies that could enhance translatability for ALS patients.

We aimed at overcoming the limitations of existing strategies for noninvasive CNS delivery, by engineering HIV-1 vectors with tropism to spinal cord MNs delivered via the neuromuscular junction (NMJ).[22] We have previously described the generation of HIV-1-based coxsackievirus and adenovirus receptor (αCAR)-targeted vector, and shown that intramuscular (i.m.) delivery of αCAR-targeted vector in mouse leg muscles results in specific retrograde transduction of lumbar MNs.[22] Our approach is based on antibody mediated cell-specific targeting and involves modification of the viral vector surface to redirect target specificity.[23] More specifically, a binding-deficient version of the α-virus Sindbis glycoprotein is used to pseudotype lentiviral vectors and to mediate fusion of viral and endosomal membrane, while the specificity is determined by an antibody (here the αCAR) chosen to recognize a specific surface receptor of the desired cell type.[23,24]

In this study, we used the αCAR-targeted LV to deliver therapeutics to SOD1^{G93A} ALS mice. We chose the human class I *IGF-1* which has previously been reported to prolong survival in transgenic mouse ALS models upon retrograde delivery from the muscle to spinal cord MNs.[12] Utilizing the αCAR-targeted LV, we investigated in vivo the neuroprotective effects of lentivirally expressed *IGF-1* for inducing neuronal survival and delaying neuropathology and behavioral phenotypes associated with the SOD1^{G93A} mouse model of ALS. Upon i.m. delivery, prior to onset of disease (day 28), αCAR *IGF-1* LV is retrogradely transported through the synapse via the axon to the nucleus of spinal MNs, where the secreted *IGF-1* can act in an autocrine manner on IGF-1 receptors on MNs to induce neuroprotective downstream signaling and/or in a paracrine on other cells. We demonstrate substantial therapeutic efficacy in vivo with αCAR *IGF-1* LV pretreatment which is linked to improved motor performance. Finally, histological analysis of spinal cord samples at end point shows that i.m. delivery of αCAR *IGF-1* LV delays disease onset and increases motor neuron survival compared with age-matched controls. This vector exhibits cross-species transduction in the rat CNS.

Methods and Materials

Production of LVs

HEK 293T cells, obtained from ATCC, were maintained in a 5% CO_2 environment in Dulbecco's modified Eagle's medium (Sigma, UK), with 10% Newborn Calf Serum (Heat Inactivated, Sigma, Dorset, UK), 1% Penicillin/Streptomycin and 1% L-glutamine (Sigma, UK). A total of 6×10^8 cells 293T cells were seeded onto a cell factory with 10 layers CF-10 (VWR, Leicestershire, UK). A DNA plasmid manufacturing company (Plasmid Factory, Bielefeld, Germany) was used for production of research grade supercoiled DNA. The complementary DNA for human insulin-like growth factor-1 (*IGF-1*) was encoding the Class 1 *IGF-1*Ea[12] was codon optimized for human and synthesized by Gene Art (Life Sciences, Paisley, UK). Thereafter, 24 h upon seeding 293T cells at 80% confluence were transfected with 0.6 mg vector plasmid (pRRLsincppt-CMV-*IGF-1*-WPRE), 0.3 mg of each of the packaging vector plasmids expressing the HIV-1 gag/pol gene (pMD2-LgpRRE), HIV-1 Rev (pRSV-Rev) (kindly provided by Professor James Uney, University of Bristol, Bristol, UK) together with 0.3 mg of each of pαIgαβ, pSINmu and pαCAR described in[22] following the addition of 2.5 mol/L $CaCl_2$. For VSVG IGF-1, LVs cells were transfected with 0.6 mg therapeutic vector plasmid (pRRLsincppt-CMV-*IGF-1*-WPRE), 0.6 mg of the packaging vector plasmid pMD2-LgpRRE, 0.12 mg of the packaging vector plasmid pRSV-Rev, and 0.3 mg the VSV-G envelope plasmids (pMD2-VSV-G). Then the 16 h posttransfection medium was replaced with fresh low serum (2%) media supplemented with 10 mmol/L sodium butyrate; 72 h posttransfection, the viral supernatant was collected and filtered through a 0.20-μm-pore size filter. Preparations were concentrated by centrifugation at 6000 rpm for 12–16 h at 4°C (Beckman Coulter Avanti J-E, F500 rotor, Beckman Coulter, High Wycombe, UK). The pellet was resuspended in ice-cold phosphate-buffered saline (PBS), and was further concentrated by ultracentrifugation for 90 min at 20,000 rpm, 10°C (Beckman Coulter Optima L-80XP). The pellet was resuspended in 300 μL ice-cold TSSM formulation buffer (20 mmol/L

Tromethamine, 100 mmol/L NaCl, 10 mg/mL sucrose and 10 mg/mL mannitol) (2000-fold concentration). Viral titer was determined as described before.[22]

Single plasmid transfections

Single plasmid lipofectamine transfections were performed utilizing the Lipofectamine LTX and Plus Reagent kit (Life Technologies, Paisley, UK). Briefly, 24 h prior to transfection HEK 293T cells were seeded onto 6-well plates (1×10^6 cells/well). Next day, an hour prior to transfection medium was replaced with low serum (2%) DMEM medium and 2.5 μg of supercoiled plasmid DNA was diluted in a mixture of OPTI-MEM solution, PLUS Reagent and LTX Reagent according to manufacturer's instructions. Transfection solution was added dropwise directly onto the cells and incubated at 37°C, 5% CO_2 for 40 h.

Western blot

For cell lysate preparation, a monolayer of packaging cells were lysed with RIPA buffer (89900, Thermo Scientific, Paisley, UK) supplemented with 1× proteinase inhibitor mixture (E1014-5KU, Thermo Scientific). Lysates were cleared by centrifuging at 15,000 rpm for 30 min at 4°C and supernatant was kept at −80°C. Prior to SDS-PAGE analysis, protein concentration in the cell lysate samples was determined by BCA (Bradford and bicinconinic Acid) Protein assay (23227, Thermo Scientific). Boiled samples in 2× SDS loading buffer were resolved on a 5–12% SDS-polyacrylamide gel (SDS-PAGE). Upon electrophoresis, the separated proteins were transferred onto a nitrocellulose membrane (Hybond-ECL, GE healthcare, Amersham, UK). The resulting blots were blocked in 5% milk solution in 1× PBS-Tween (0.1% v/v) overnight at 4°C. The next day the blots were incubated with relevant primary antibodies. To detect the HA tag, blots were incubated with anti-HA-HRP (1: 5000 in 5% milk PBS-Tween 0.1% v/v, Miltenyi Biotec) for 1.5 h at room temperature. To detect human IGF-1, membranes were incubated with goat anti-human *IGF-1* (2 μg/mL in 5% milk PBS-Tween 0.1% v/v, ab106836 Abcam, Cambridge, UK) for 1.5 h at room temperature. Mouse mAb to GAPDH protein (1:1000, Santa Cruz, Heidelberg, Germany) was used as loading control. Secondary antibodies used were a 1:3000 or (in 0.5% milk PBS-Tween 0.1% v/v) of relevant HRP-linked anti-IgG, followed by detection, using ECL reagent (Pierce, Thermo Scientific).

Enzyme linked immunosorbent assay of human IGF-1

Protein from animal tissue was isolated by rapidly dissecting the tissue on ice and immediately homogenizing, using either the RIPA buffer (89900, Thermo Scientific) or the Tissue Protein Extraction Reagent (Pierce, Rockford, IL) supplemented with 1× proteinase inhibitor mixture (E1014-5KU, Thermo Scientific). Enzyme-linked immunosorbent assay for human *IGF-1* was performed in duplicate, using the Duo Set ELISA kit (DY291; R&D Systems, Abingdon, UK) in combination with MSD platform (Mesoscale Diagnostics, MD, Maryland, USA). Protein homogenates were diluted 2000-fold for cells and twofold for tissue, using the assay diluent and the assays performed following the MSD recommendations.

Animals

All animal procedures were approved by the local Ethical Committee and performed in accordance with United Kingdom Animals Scientific Procedures Act (1986) and associated guidelines. All efforts were made to minimize the number of animals used and the suffering. Animals were supplied by Charles River, UK and housed under a 12 h light/dark cycle with food and water available ad libitum.

The congenic C57BL/6J Tg (SOD1 G93A)1Gur(G93A-SOD1) mice (Jackson Laboratory, Bar Harbor, ME) were used[25] and were backcrossed onto the wild-type C57BL/6 mouse background (Charles River Laboratories, Wilmington, MA) for >10 generations. A priori power analysis revealed that 12 animals per group (both males and females) was a sufficient sample size in order to detect a medium effect with 80% power.[26] Transgenic mice were genotyped according to the Jackson Laboratory protocols and were organized in subgroups of 18 (6 animals per group; (i) no treatment or mock (αCAR *eGFP* LV), (ii) αCAR *IGF-1* LV, (iii) VSVG *IGF-1* LV), and they were age matched and litter matched wherever possible. Human $SOD1^{G93A}$ gene copy number was assessed[27] and remained stable across generations (Copy number 25+/-1.2 copies $hSOD1^{G93A}$; remained stable across mice used, F3–F6). We found only one mouse with an altered SOD1 gene copy number and this mouse was removed from the study.

LV delivery

For mice injections, a total volume of 100 μL of lentiviral vector solution was delivered via single bilateral intramuscular injection (28 days of age ± 1 day) in key muscle groups (gastrocnemius muscle [GA], 20 μL; tibialis anterior muscles (TA), 15 μL; intercostal muscles 10 μL; triceps muscles 5 μL) with a micro-fine 29G insulin needle, under general anesthesia with isofluorane.

For weight, survival, rotarod, and a catwalk performance, 60 $SOD1^{G93A}$ mice (αCAR *IGF-1* LV: $n = 24$ in

total, $n = 12$ males, $n = 12$ females; VSVG *IGF-1* LV: $n = 12$ in total, $n = 6$ males, $n = 6$ females; no treatment: $n = 12$ in total $n = 6$ males, $n = 6$ females; αCAR *eGFP* LV: $n = 12$ in total, $n = 6$ males, $n = 6$ females) were assessed. For motor neuron counts 16 $SOD1^{G93A}$ mice (αCAR *IGF-1* LV: $n = 8$ in total, $n = 4$ males, $n = 4$ females; VSVG *IGF-1*: $n = 8$ in total, $n = 4$ males, $n = 4$ females; αCAR *eGFP* LV: $n = 4$ in total; $n = 2$ males, $n = 2$ females; no treatment: $n = 4$ in total; $n = 2$ males, $n = 2$ females) were assessed.

Because αCAR *eGFP* LV and nontreated mice had the same survival and performed equivalently on the behavioral assessments they were presented in analysis as one group named as nontreated ($n = 24$; $n = 12$ males, $n = 12$ females).

For intrastriatal injections in rats, in vivo application of αCAR-targeted vector and control in CNS was performed to examine the neurotropism of the lentiviral preparations. In in vivo intrastriatal applications, male Wistar rats, weighing 200–250 gr were used. Animals were placed in a stereotactic frame (Taxic-6000, World Precision Instruments, Hitchin, UK) with the nose bar set at −3.3 mm under general anesthesia. The scalp was cut and retracted to expose the skull. Craniotomy was performed by drilling directly above the target region, to expose the pial surface. One single injection was directed into the right striatum using the stereotactic coordinates relative to bregma: anteroposterior, 0.5 mm; mediolateral, 3.0 mm; dorsoventral, 5.0 mm. Animals usually received 4.0 μL of pseudotyped LV vectors with a biological titer within the scale of 1×10^9 TU/mL via a 32G blunt needle, using an infusion pump (UltramicropumpIII and Micro4 Controller, World Precision Instruments) at a stable flow rate of 0.2 μL/min over 20 min. Upon delivery, needle was allowed to remain on site for additional 5 min prior to slow retraction.

Behavioural and survival analysis

Behavioral assessment and all in vivo tests were carried out from 65 days of age until 150 days of age blinded to treatment. All animals were weighted weekly until they reached 110 days of age at which point they were weighted daily until end stage. Motor coordination and performance were recorded using the Ugo Basile ROTA-ROD for mice (Ugo Basile, Varese, Italy). Each weekly session consisted of three trials on the rotarod, which was set to accelerate from 5 rpm (rotations per minute), and the latency to fall was recorded in seconds. The maximum time depicting no motor impairment was defined as 300 sec. The time each mouse remained on the rod was registered. Footprint analysis was also performed every 10 days. Mouse hind- and fore-paws were covered with red and green paint, respectively, to record walking patterns during continuous locomotion, and stride length was measured. Gait analysis was also performed using the automated footprint recording Catwalk system 10.5 (Noldus Information Technology, Wageningen, The Netherlands) every 10 days. Briefly, each animal was allowed to run from one side of the glass plate to the other and a camera placed underneath the glass plate recorded the video image of each run. Survival analysis was performed using the Kaplan–Meier survival analysis. End stage was defined the point at which the animals could no longer "right" themselves within 30 sec after being placed on their back.

Perfusion and tissue processing

When mice reached the endpoint (loss of righting reflex for 30 sec), they were killed by intraperitoneal injection of 200 mg/kg of sodium pentobarbitone, and then transcardially perfused with 20 mL saline (0.9% w/v NaCl) supplemented with heparin 5 units/mL (Sigma) followed by 20 mL of 4% (w/vol) paraformaldehyde (PFA, Sigma Aldrich) in PBS. Spinal cord, TA, *GA*, *intercostal,* and *triceps* muscles were removed and either postfixed for 4 h in 4% PFA, followed by cryoprotection in 10% glycerol and 20% sucrose in PBS for at least 72 h or snap frozen in liquid nitrogen and stored at −80°C until further analysis. Fixed tissues were subsequently embedded and frozen in OCT (Surgipath FSC22; Leica Microsystems, Wetzlar, Germany). Twenty micrometer coronal sections from the sacral plexus through the entire lumbar and thoracic parts of the spinal cord were cut using a cryostat (Leica Microsystems), mounted on gelatinized slides, and stored at −20°C.

For western blot analysis upon euthanasia, mice were perfused with 20 mL saline (0.9% w/v NaCl) plus heparin. The same tissues, as mentioned above, were removed and snap frozen using liquid nitrogen.

Rats were killed 3 weeks postinjection by intraperitoneal injection of 200 mg/kg of sodium pentobarbitone, transcardially perfused with 200 mL saline (0.9% w/v NaCl) plus heparin, followed by 250 mL of 4% PFA in PBS. Brains were removed and postfixed for 4 h in 4% PFA, followed by cryoprotection in 10% glycerol and 20% sucrose in PBS for at least 72 h. The brain was subsequently embedded and frozen in OCT (Surgipath FSC22; Leica Microsystems).

Motor neuron quantification

Sections were processed for cresyl violet staining stain (0.1% Cresyl Fast Violet; BDH, Lutterworth, UK). Surviving motor neurons were counted in every 10th section under a light microscope at ×20 magnification in order to avoid repetitive counting ($n = 24$ mice [eight per group]). MN counting was performed blindly between different groups and sexes. Only motor neurons with a

clearly identifiable nucleus and nucleolus and a cell soma were counted. MN quantification was performed in spinal cord sections extracted from animals at end stage.

Immunohistochemisty

Immunohistochemistry was performed on slide mounted spinal cord sections. Tissue was permeabilized for 1 h with PBS-containing 10% donkey serum and 0.1% Triton-X100. Antibodies to eGFP (1:500, ab290, Abcam), ChAT (1:50 AB114P, Millipore, Watford, UK) were diluted in the same buffer and placed on sections for 72 h at 4°C. Sections were then blocked for 30 min prior to incubating for 3 h at room temperature with donkey anti-rabbit, anti-goat secondary antibodies conjugated with AlexaFluor® 488 or 594 (1:500; Invitrogen, Paisley, UK), respectively. Sections were mounted with ProLong anti-fade aqueous mounting medium (Invitrogen).

For rat brain tissue, 30 μm coronal sections from the olfactory bulb (OB), through the entire striatum, globus pallidus and substantia nigra (SN) were cut using a cryostat (Leica Microsystems), mounted on poly-L-lysine coated slides, and stored at −20°C. Immunohistochemistry was performed on slide mounted brain sections. The tissue was permeabilized and blocked for 1 h with PBS-containing 10% donkey serum and 0.1% Triton-X100. Primary antibodies to eGFP (1:500, ab290, Abcam), NeuN (1:100, MAB377, Millipore) and GFAP (1:400, MAB360, Millipore) were diluted in the same buffer and applied on sections for 48 h at 4°C. Sections were then washed three times with PBS for 10 min, shaking gently and blocked for 30 min prior to incubation with secondary fluorescently labeled antibodies (for 3 h at room temperature). ProLong anti-fade aqueous mounting medium with DAPI was used to apply coverslips (Invitrogen).

Statistical analysis

Survival analysis of the SOD1^{G93A} mice was performed by Kaplan–Meier analysis, which generates a χ^2 value to test for significance. All other tests not involved in survival analysis were performed by multi-way analysis of variance followed by a Bonferroni post hoc analysis of means differences between groups (GraphPad Prism Software, San Diego, CA).

Results

Generation of αCAR IGF-1 and control LVs

In the current study we utilized the αCAR-targeted lentiviral vector (αCAR-targeted LV) to deliver therapeutics to SOD1^{G93A} mice. We chose the human class I Insulin like growth factor 1 (*IGF-1*Ea), which has previously been reported to prolong survival in transgenic mouse ALS models through viral mediated delivery applied distally.[12,14,16] Towards this end we cloned a codon-optimized version of the human class 1 *IGF-1* (class 1 *IGF-1*Ea) into an HIV-1-based lentiviral vector under the control of the human cytomegalovirus (CMV) enhancer and promoter (Fig. 1A). We inserted an HA tag on the 5 prime end of *IGF-1*. As a control we used αCAR-targeted LV vector expressing the enhanced green fluorescent protein (eGFP), a system which was previously found and reconfirmed here using cell factory preparations to be effective for targeted expression in spinal cord MNs after TA injections[22] (Fig. 1A). Human IGF-1 expression was assessed via western blot in total protein extracts following lipofectamine transfections of either the pRRLsincppt-CMV-*IGF1*-WPRE therapeutic or the pRRLsincppt-CMV-*eGFP*-WPRE construct in HEK293T cells (Fig. 1B). Human IGF-1 levels were measured in homogenates and supernatant of cells transfected with HIV-1 *326-pRRLsincppt-CMV-IGF-1-WPRE* and *326-pRRLsincppt-CMV-eGFP-WPRE* plasmids using an enzyme-linked immunosorbent assay (ELISA) that recognized the expressed human IGF-1 (Fig. 1C). Detectable levels of human IGF-1 were noted in both homogenates (>2 μg/μL) and supernatant (>1 μg/μL) of cells transfected with the therapeutic expression plasmid *pRRLsincppt-CMV-IGF-1-WPRE.* Highest levels were found in homogenates of cells transfected with *pRRLsincppt-CMV-IGF-1-WPRE.* Negligible levels of human IGF-1 were detected only in the lysates of cells transfected with the control *326-pRRLsincppt-CMV-eGFP-WPRE* expression plasmid, with background levels detected <20 ng/μL.

To assess the expression levels of lentivirally expressed *IGF-1* we infected HEK 293T cells with LVs expressing the human *IGF-1* at MOI 50. Cells transduced with LVs expressing eGFP were used as control. Using an ELISA we were able to detect human IGF-1 in lysates (mean IGF-1 levels 732.14 ng/mL) and secreted IGF-1 in the supernatant of cells transduced (mean IGF-1 levels 7591.88 ng/mL) with LVs expressing the human *IGF-1* (Fig. 1D). No IGF-1 was detected in either lysates or supernatants of cells transduced with control eGFP-expressing LVs (mean background levels at 220.15 ng/mL for cell lysates).

These data demonstrate that the synthetic human *IGF1-Ea* we cloned in HIV-1 is efficiently expressed and secreted upon infection of HEK293T cells with *IGF-1*-expressing LVs.

We subsequently generated a therapeutic αCAR-targeted LV encoding the same secretable codon-optimized human *IGF-1* under the same promoter. By utilizing cell factories we produced high titer preparations of therapeutic-targeted αCAR *IGF-1* LVs. We also produced Vesicular Stomatitis Virus glycoprotein (VSV-G) pseudotyped LVs

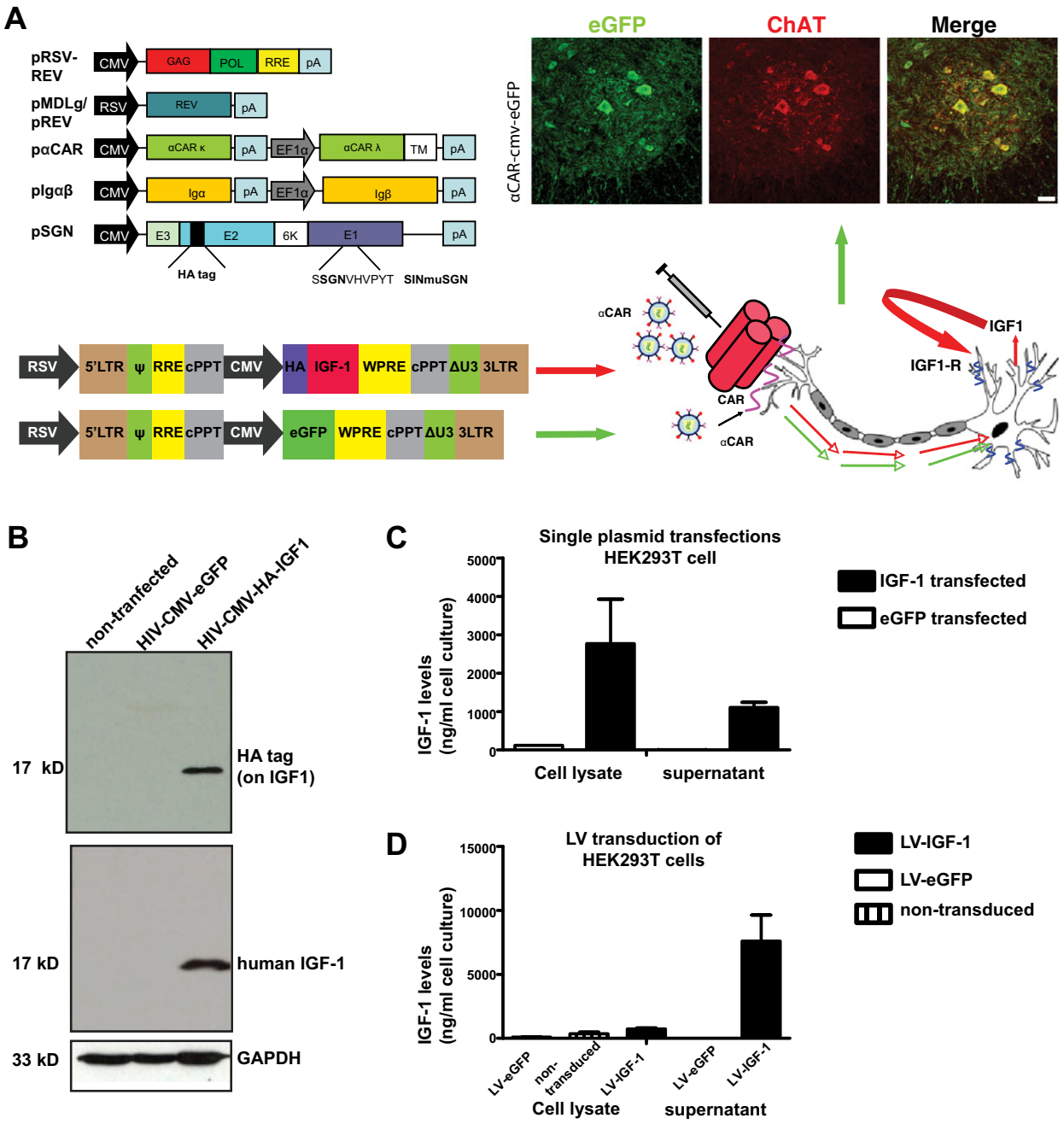

expressing human *IGF-1* to assess neuroprotection resulting from muscle-produced IGF-1.

Intramuscular delivery of αCAR *IGF-1* LV prolongs survival of SOD1^{G93A} animals

To investigate the neuroprotective effects of αCAR *IGF-1* LV on ALS pathogenesis, we performed single bilateral delivery of either αCAR-targeted or control VSV-G pseudotyped LVs expressing *IGF-1* into key muscle groups of both male and female SOD1^{G93A} mice (n = 24 animals/group) predisease onset at 28 days of age (Table S1). Impact of the different treatments on survival of SOD1^{G93A} mice was analyzed by Kaplan–Meier survival curves. Treated mice were monitored up to end stage and compared with control groups. Onset of disease (measured by weight loss from denervation-induced muscle atrophy) was significantly delayed by a median of 32 days in αCAR *IGF-1*-treated mice when compared with nontreated control mice (Fig. 2A; nontreated, 118.5 days;

Figure 1. Generation and characterization of targeted lentiviral vectors. (A) Experimental design for overexpression of IGF-1 or eGFP in MNs of SOD1^{G93A} mice. Schematic drawing of the plasmids used for production of spinal cord MN-targeted αCAR LVs produced in cell factories. αCAR-targeted vectors were generated by six-plasmid co-transfection using the pMD2-LgpRRE and pRSV-Rev packaging plasmids, the pαCAR plasmid, Igαβ plasmid required for surface expression of antibody molecules, SINmu(SGN) envelope plasmid, and the pRRLsincppt-CMV-*IGF-1*-WPRE or pRRLsincppt-CMV-*eGFP*-WPRE genome plasmid in HEK293T cells. The human codon optimized sequence that encodes the class 1 insulin-like growth factor-1, *IGF-1*Ea was cloned into the pRRLsincppt-CMV-WPRE HIV-1 genome plasmid under the control of human cytomegalovirus (CMV) immediate early enhancer and promoter. Following uptake by CAR receptors at the NMJ vectors become retrogradely transported and transduce spinal motor neurons either with eGFP or *IGF-1* which following secretion binds at surface expressed receptors and activates downstream signaling cascades mediating neuroprotection. eGFP expression following injection into TA muscle of mice results in specific retrograde transduction of MNs in dorsolateral nucleus in L3-L5 of spinal cord. Scale bar: 50 μm. (B) Western blot analysis of total protein extracts following lipofectamine transfections of pRRLsincppt-CMV-*IGF1*-WPRE therapeutic or pRRLsincppt-CMV-*eGFP*-WPRE control construct in HEK293T cells. Cell lysates of transfected HEK293T cells and nontransfected controls were subjected to lysates from nontransfected cells and cells transfected with pRRLsincppt-CMV-*eGFP*-WPRE construct, both lacking the human *IGF-1* and the HA-tag, served as controls. Human *IGF-1* (middle panel) and HA tag (top panel) were, as expected, detected in lysates of cells transfected only with the targeted therapeutic constructs. Lower panel: Loading control. (C) Human *IGF-1* levels in homogenates and supernatant of cells transfected with HIV-1 *pRRLsincppt-CMV-IGF-1-WPRE* and *pRRLsincppt-CMV-eGFP-WPRE* plasmids were measured by enzyme-linked immunosorbent assay. (D) Human IGF-1 levels in homogenates and supernatant of cells transduced with LVs expressing either eGFP or human *IGF-1*Ea or genes at an MOI 50 and noninfected cells were measured by enzyme-linked immunosorbent assay. CAR, coxsackievirus and adenovirus receptor; CMV, cytomegalovirus promoter; eGFP, enhanced GFP; R, HIV-1 viral protein R; LTR, long-term repeats; Ψ, Retroviral Psi packaging element; RRE, HIV-1 Rev response element; cPPT, central polypurine tract; WPRE, woodchuck hepatitis virus posttranscriptional regulatory element; ΔU3, mutated viral enhancer region.

$P < 0.0001$ Wilcoxon, signed-rank test) and by 9 days when compared with VSVG *IGF-1*-treated mice (Fig. 2A; VSVG *IGF-1*-treated, 141.5 days $P = 0.0133$, Wilcoxon signed-rank test). When male αCAR *IGF-1*-treated SOD1^{G93A} cohorts were analyzed separately disease onset was significantly delayed by 29.5 days when compared with nontreated control male mice (Fig. S1A; 145 vs. 115.5 days $P < 0.0001$ Wilcoxon, signed-rank test) and by 6 days versus VSVG *IGF-1*-treated mice; however, the later delay was not significant. In the female cohorts, treatment with αCAR *IGF-1* significantly delayed disease onset by 32.5 days when compared with nontreated control female mice (Fig. S1; 153 vs. 120.5, $P < 0.0001$) and by 9 days when compared with VSVG *IGF-1*-treated mice (Fig. S1; 153 vs. 144, $P = 0.0087$). We observed an 8-day difference in median disease onset between female and male αCAR *IGF-1* LV-treated cohorts, however this difference was not significant (females: 153 days vs. males: 145 days; $\chi^2 = 1.711$, $P = 0.1908$).

Survival analysis showed that mice treated with targeted therapeutic αCAR *IGF-1* LV showed a 14-day increase in median lifespan when compared with nontreated control mice (Fig. 2B; 169 vs. 155; log-rank test, $\chi^2 = 18.15$, $P < 0.0001$) and 9 days when compared with VSVG *IGF-1*-treated mice (Fig. 2B; 169 vs. 160; log-rank test, $\chi^2 = 6.308$, $P = 0.012$). There was no difference in survival between nontreated and VSVG *IGF-1*-treated control mice. When male and female cohorts were analyzed separately αCAR *IGF-1* LV treatment significantly increased median lifespan in both male and females when compared with nontreated control cohorts by 12 and 8 days (Fig. S1B; males, log-rank test, $\chi^2 = 8.513$, $P = 0.0035$; females $\chi^2 = 7.913$, $P = 0.0049$), respectively. When αCAR *IGF-1* LV-treated cohorts were compared with VSVG *IGF-1*-treated male and female mice, median lifespan was significantly increased in both female and male mice (Fig. S1B; females: 7.5 days; log-rank test, $\chi^2 = 4.756$, $P = 0.0292$; males: 4 days; log-rank test, $\chi^2 = 4.518$, $P = 0.0335$). When we compared median survival between female and male αCAR *IGF-1* LV-treated cohorts, we found no significant difference (females: 168 days vs. males: 170 days; log-rank test, $\chi^2 = 0.1008$, $P = 0.7509$).

Interestingly we observed some variability in survival with two female mice surviving up to 197 and 198 days and 1 male mouse up to 240 days, which accounts for extension of survival of up to 27% and 54%, respectively, compared with VSVG *IGF-1* LV and nontreated controls.

Weekly body weight measurements revealed a significantly slower loss of body weight in αCAR *IGF-1*-treated mice from 135 days onward. P28 αCAR *IGF-1* LV-treated female mice maintained their weights when compared with age-matched controls (Fig. 2C). More specifically, αCAR *IGF-1* LV treatment significantly delayed weight decline at days 136–145 when compared to nontreated controls and at days 152 ($P < 0.1$) and from day 155 onwards ($P < 0.001$) when compared with VSVG *IGF-1* LV-treated mice. In male mice αCAR *IGF-1* LV treatment significantly delayed weight decline compared with nontreated male mice from day 145 ($P < 0.01$), but no significant effect was found versus the VSVG *IGF-1* LV-treated male control mice (Fig. 2D).

αCAR *IGF-1* LV improves motor function and coordination in SOD1^{G93A} mice

Motor performance, coordination and gait analysis were assessed weekly from day 65 onwards, for both *IGF-1*-treated and control groups (Fig. 3). SOD1G93A mice were

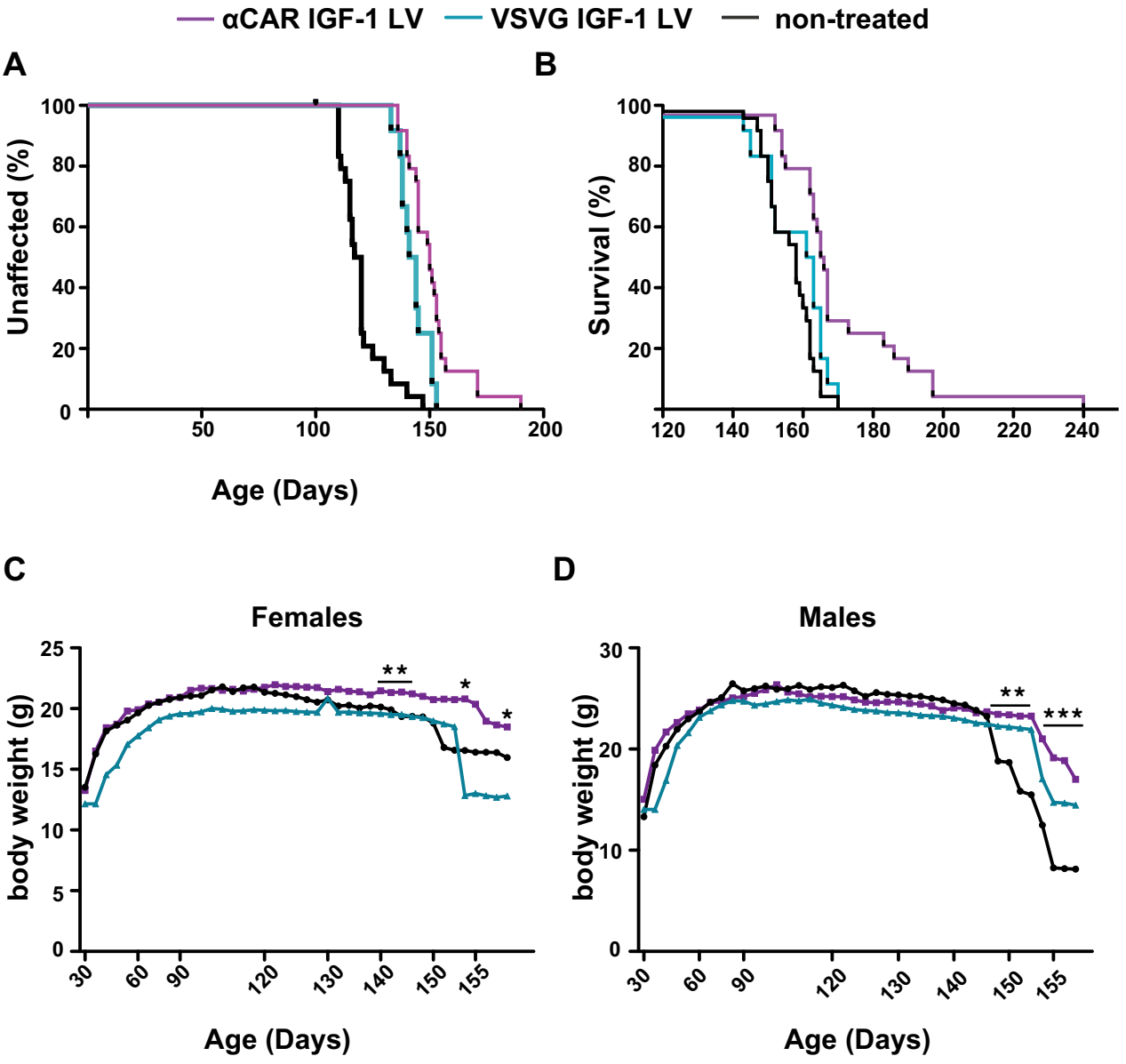

Figure 2. αCAR *IGF-1* LV improves survival in SOD1^{G93A} mice. (A) Kaplan–Meier survival analysis of αCAR *IGF-1* LV and VSVG *IGF-1* LV-treated and nontreated control female and male SOD1^{G93A} mice. Treated mice were monitored up to end-stage and compared to nontreated control group. End stage was defined as the point at which the animals could no longer "right" themselves within 30 sec after being placed on their back. Survival analysis showed that the median lifespan of SOD1^{G93A} mice was extended by 8 days in αCAR-*IGF-1* LV-treated mice (Kaplan–Meier plot; $n = 12$ mice per group, $P < 0.001$, $\chi^2 = 14.92$). (B) Comparison of mean age of survival in all groups. Mean survival was significantly improved in αCAR *IGF-1* LV-treated compared with both control groups (one-way ANOVA, Tukey's Multiple Comparison Test, $P < 0.05$) (C) P28 αCAR *IGF-1* LV-treated female mice maintained their weight compared with age-matched controls. αCAR *IGF-1* LV significantly delayed weight decline compared with nontreated controls at days 136, 140–145 (**$P < 0.01$) and at day 160 and onwards (*$P < 0.05$) and compared to VSVG *IGF-1* LV-treated mice at days 152 (*$P < 0.05$) and from d155 onward (*$P < 0.05$). (D) Compared to VSVG *IGF-1* LV-treated male mice controls, αCAR *IGF-1* LV had no effect on weight decline. αCAR *IGF-1* LV significantly delayed weight decline compared to nontreated males mice from day 145 (**$P < 0.01$, ***$P < 0.001$). αCAR *IGF-1* LV-treated mice ($n = 24$) are shown in magenta, VSVG-*IGF-1* LV-treated mice ($n = 12$) are shown in light blue and nontreated control group in black.

tested weekly for rotarod coordination and their performance was analyzed over time for female ($n = 12$ per group) and male ($n = 12$ per group) cohorts (Fig. 3A). Rotarod tests showed that αCAR *IGF-1* LV-treated female mice maintained their ability to coordinate their movement for a longer period than both VSVG *IGF-1*-treated

and nontreated mice starting from 130 days until end stage ($P < 0.05$ from 130 days of age onward, $n = 12$ animals per group). However, αCAR *IGF-1* LV-treated male mice had significantly better rotarod performance than nontreated control animals starting from 130 days onward ($P < 0.05$, $n = 12$ animals per group), but no significant difference was observed between αCAR *IGF-1* LV and VSVG *IGF-1* LV-treated male mice. Manual footprint analysis showed impaired walking patterns in control animals compared with aged-matched αCAR *IGF-1* LV-treated mice from 115 days onwards ($P < 0.05$, from 115 day onward, $n = 12$ animals per group) (Fig. 3B). Representative walking patterns from manual footprint analysis are presented in Figure S2B. Results were confirmed on a separate cohort of mice where digital footprint analysis also demonstrated impaired walking patterns in control animals compared with aged-matched αCAR *IGF-1* LV-treated mice, but this time from 125 days onwards (Fig. 3C). Representative footprints of late symptomatic stage mice showed that nontreated $SOD1^{G93A}$ mice dragged their hind legs, whereas αCAR *IGF-1* LV-treated mice showed minor defects in coordination of steps (Fig. S2A).

Overall, the administration of MN-targeted αCAR *IGF-1* LV significantly delayed the onset of disease as assessed by rotarod performance tests, gait analysis and body weight compared with nontreated and VSVG *IGF-1* LV-treated control $SOD1^{G93A}$ mice. Interestingly, there was no statistical difference observed between male mice treated with αCAR *IGF-1* LV and VSVG *IGF-1* LV in both rotarod test and body weight assessment other than one time point at 155 days of age in body weight measurements of surviving mice (Fig. 2D).

Intramuscular application of αCAR *IGF-1* LV resulted in motor neuron protection in $SOD1^{G93A}$ mice

ALS has been associated with progressive and severe spinal motor neuron atrophy and cell death.[28] Targeted αCAR *IGF-1* LV was assessed for its ability to exert a neuroprotective effect and consequently increase motor neuron survival in $SOD1^{G93A}$ mice compared with nontreated control animals when applied preonset of disease at 28 days of age. Lumbar and thoracic regions of spinal cord were labeled and evaluated for surviving MNs at end stage. MNs were identified by their location within the spinal cord, their morphology and their size. Histological evaluation of end-stage lumbar spinal cord samples revealed loss and atrophy of MNs in nontreated mice (Fig. 4A top panel and Fig. 4B) and VSVG *IGF-1* LV compared with large-sized surviving MNs observed in αCAR *IGF-1* LV-treated $SOD1^{G93A}$ mice (Fig. 4A lower panel). Surviving MNs in treated animals appeared dark stained after labeling with Nissl dye, with a lighter stained nucleus and a very dark and well-defined nucleolus. Gene transfer at end-stage αCAR eGFP injected $SOD1^{G93A}$ mice was assessed by confocal microscopy and was evident mainly in axons and less so in some of the remaining motor neurons of ventral horn (Fig. 4B). To assess survival of MNs we performed total cell counts of surviving MNs in both thoracic and lumbar parts of spinal cord obtained from nontreated, VSVG *IGF-1* LV and αCAR *IGF-1* LV-treated animals at end-stage of the disease (both male and females). αCAR *IGF-1* LV-treated animals showed a significant preservation of MNs in the lumbar part of the spinal cord compared with both nontreated and VSVG *IGF-1* LV mice (mean MN counts 18.55 ± 1.22 vs. 12 ± 2.12 and 6.80 ± 1.20, respectively, $P = 0.0026$) (Fig. 4C). αCAR *IGF-1* LV-treated animals displayed higher numbers of surviving MNs per section compared with nontreated and VSVG *IGF-1* injected mice (mean MN counts 17.43 ± 1.44 vs. 10 ± 1.12 and 6.85 ± 1.75, respectively; $P = 0.018$) also in the thoracic region of the spinal cord (Fig. 4C). To determine whether survival of spinal cord MNs was due to neuroprotection derived from lentivirally expressed *IGF-1* we measured the levels of human IGF-1 in homogenates of end-stage lumbar spinal cord samples from nontreated and αCAR *IGF-1* LV-treated animals. Toward this end, we used an ELISA that recognized the expressed human IGF-1 and not the endogenous murine one. Detectable levels of human IGF-1 were found in the spinal cord of αCAR *IGF-1* LV-treated mice (mean IGF-1 levels 18.736 ng/mg), while little to no IGF-1 was detected in nontreated animals, with mean background levels at 2.1 ng/mg (Fig. 4D).

Cross-species neuronal transduction of αCAR LV

To further investigate the in vivo tropism of the αCAR-targeted vector and investigate its ability to be retrogradely transported, αCAR-targeted and control vectors were stereotaxically applied to the rat striatum. Details of the lentiviral preparations produced for striatal injections are presented in Table S2. Prior to the injection, vectors were normalized to vector infectivity values to ensure equal administration of potent lentiviral particles. All rats received 4 μL of appropriate lentiviral preparation diluted in formulation buffer (TSSM). Three weeks postinjection the animals were euthanized and brains were examined for eGFP expression, indicative of retrograde delivery and expression of the transgene by the HIV-1-based αCAR-targeted LV. Figure S3 shows that the αCAR-targeted vector efficiently delivers the transgene to the site of injection showing considerable affinity for neurons, though still transducing a small amount of astroglia. The nontargeted

Figure 3. αCAR *IGF-1* LV significantly prolonged motor performance in $SOD1^{G93A}$ mice. (A) SOD1G93A mice were tested weekly for rotarod coordination. The rotarod performance was analysed over time of either only females (n = 12 per group), or only males (n = 12 per group) cohorts. αCAR *IGF-1* LV-treated female mice had better rotarod performance as compared with age-matched controls from 130 days onwards (two-way ANOVA, Bonferroni post hoc test, $***P < 0.001$, $*P < 0.05$; error bars represent ± SEM). αCAR *IGF-1* LV-treated male mice had better rotarod performance as compared with age-matched nontreated controls from 130 days onwards (two-way ANOVA, Bonferroni post hoc test, $*P < 0.05$; error bars represent ± SEM). No significant difference was observed between αCAR *IGF-1* LV and VSVG *IGF-1* LV-treated male mice. (B) Dynamic parameters of gait analysis using manual footprint analysis. Stride length is the distance in millimeters between successive placements of the same paw. Footprint analysis showed impaired walking patterns in control animals compared to aged-matched P28 αCAR *IGF-1* LV-treated mice from 115 days onwards (data represent average values per group ± SEM (n = 6 per group); two-way ANOVA, Bonferroni post hoc test, $**P < 0.01$, $***P < 0.001$). (C) Dynamic parameters of gait analysis using digital footprint analysis. Impaired walking patterns in control animals compared to aged-matched from 125 days onwards (data represent average values per group ± SEM (n = 6 per group); two-way ANOVA, Bonferroni post hoc test, $*P < 0.05$, $***P < 0.001$). αCAR *IGF-1* LV-treated mice (n = 24; 12 males and 12 females) are shown in magenta, VSVG *IGF-1* LV-treated mice (n = 12; 6 males and 6 females) are shown in light blue and nontreated (n = 24; 12 males and 12 females) control group in black.

control vector (lacking the targeting antibody but still pseudotyped with neurotropic sindbis-G) did also transduce neurons, however, at lower efficacy as it bears detargeting mutations. The αCAR-targeted vector resulted in retrograde transduction of mytral cells of the OB, a distal structure connected to the striatum's olfactory tubercle, as previously observed by us for other retrogradely transported vectors.[29] No significant transduction of thalamic nuclei, or pars compacta of the SN was observed though, which was probably due to the absence of vector uptake at thalamostriatal and nigrostriatal nerve terminals presumably due to the absence of aCAR receptors in those neuronal synapses.

In summary, we observed substantial therapeutic efficacy in vivo with MN-targeted αCAR *IGF-1* LV pretreatment with significant delay of disease onset and extension of survival compared with both VSV-G *IGF-1* LV and nontreated control animals linked to increased survival of MNs. Efficacy is linked to improved motor performance, as αCAR *IGF-1* LV-treated mice retained muscle tone and motor function during their prolonged survival.

Discussion

In this study, we report proof of concept studies testing a novel-targeted LV-expressing *IGF-1* for noninvasive neuroprotective gene therapy for ALS. *IGF-1* is known to have a neurotrophic effect on motor neurons.[30] To date *IGF-1*-based therapies have little beneficial effect upon systemic or intrathecal administration in ALS patients.[19–21] The poor outcomes of these studies may possibly be due to low availability of *IGF-1* as free *IGF-1* is reduced while *IGF-1*R expression is upregulated in both the CNS and muscle of ALS patients.[31,32] Alternative to these approaches, many studies have focused on distal targeting of MNs delivering therapeutics through the retrograde route. Indeed, *IGF-1* has previously been reported to prolong survival in transgenic mouse ALS models through viral mediated delivery applied distally,[12,14,16] while direct spinal cord application has had poor outcomes.[17,18] We previously showed that in vivo i.m. delivery of αCAR-targeted vector in mouse leg muscles results in specific retrograde transduction of lumbar MNs.[22] In the current study, we utilized the αCAR-targeted vector and investigated the in vivo neuroprotective effects of lentivirally expressed *IGF-1* following intramuscular application to $SOD1^{G93A}$ mice.

Specifically, we showed that we can produce high titer preparations of αCAR-targeted LVs that efficiently express human *IGF-1*. Utilising ELISA we confirmed expression of human *IGF-1* only in lysates and supernatant of cells transduced with LVs expressing this factor. Background levels detected were at least 5 to 20 orders of magnitude lower than therapeutic LV transduced cells, showing that synthetic human IGF1-Ea is successfully expressed and mature *IGF-1* is secreted upon transduction of HEK293T cells with LVs.

The results of this study indicate that *IGF-1* trophic factor delivery to CNS via a one-time i.m. application of αCAR *IGF-1* LVs has significant therapeutic benefit and can modify disease progression in the $SOD1^{G93A}$ mice. The advantage of our delivering strategy over existing approaches resides on high targeting specificity of the LVs applied distally which overcomes the need of direct injection into the spinal cord where the affected MNs reside. Recently a study utilising AAV encoded microRNA against human SOD1 has shown that suppressing SOD1 in MNs either by intracerebroventicular or by lumbar intrathecal injections can be neuroprotective.[33] In vivo i.m. application of our targeted therapeutic vector resulted in human IGF-1 protein expression in the spinal cord (Fig. 4), which in turn significantly delayed disease onset and increased mean survival of $SOD1^{G93A}$ mice by 14 days. Efficacy observed was linked to improved motor performance, as αCAR *IGF-1* LV-treated animals retained muscle tone and motor function during their prolonged survival. Our current findings are in agreement with similar studies showing that treatment with this isoform of *IGF-1* is beneficial.[11,12] Similar to others[14,16] we observed some variability in survival as not all cohorts of mice

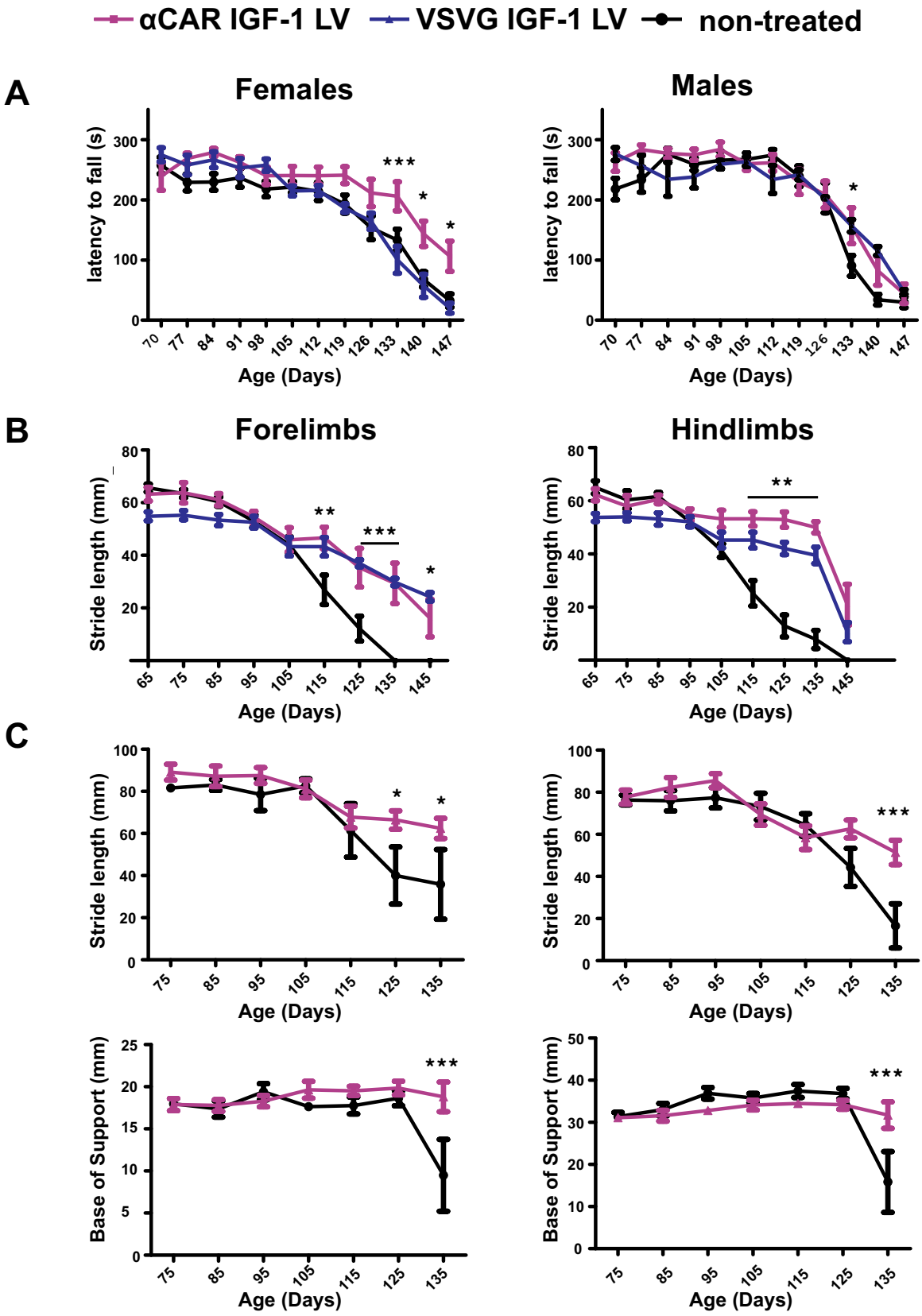

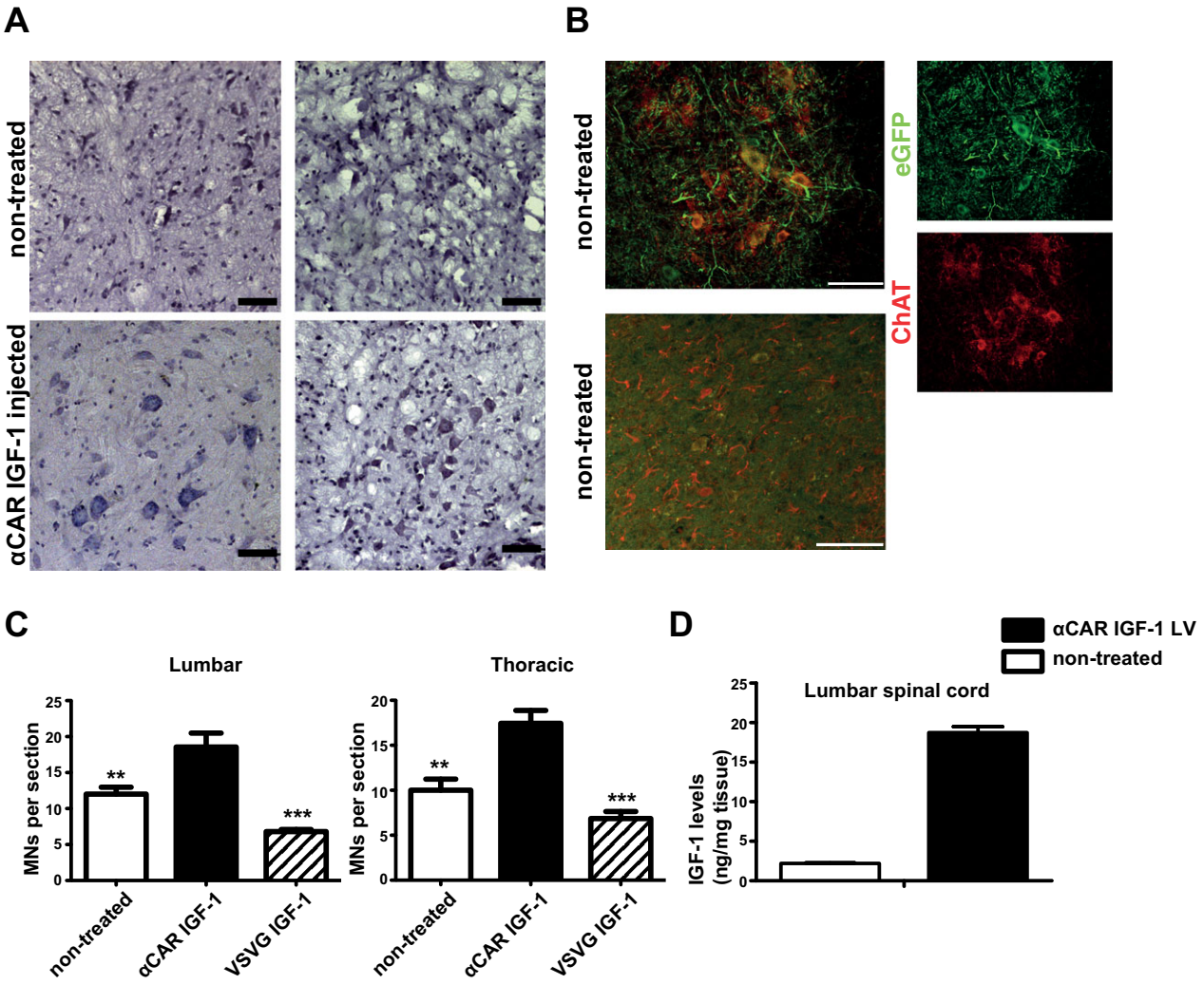

Figure 4. αCAR *IGF-1* LV protects motor neurons in SOD1^{G93A} mice. (A) Histological evaluation of end-stage lumbar spinal cord in nontreated (top panel) and αCAR *IGF-1* LV-treated (bottom panel) SOD1^{G93A} mice. Scale bars 100 μm. (B) Expression of EGFP in spinal cords of two different end-stage mice injected with the αCAR *eGFP* LV. Images show the variability observed in MN loss. Scale bars 100 μm. (C) Quantification of surviving MNs in thoracic and lumbar spinal cord in nontreated, VSVG *IGF-1* LV and αCAR *IGF-1* LV-treated animals at end-stage classification of the disease (one-way ANOVA, Tukey's Multiple Comparison Test, $P < 0.05$; error bars represent ± SEM; $n = 8$ per group). (D) Human IGF-1 levels in homogenates of end-stage lumbar spinal cord samples from nontreated (untreated) and αCAR *IGF-1* LV-treated animals were measured by ELISA. Intramuscular delivery of αCAR *IGF-1* LV resulted in human IGF-1 expression in spinal cord. Control mice showed no expression of the human IGF-1 protein.

(regardless of sex) responded equally to i.m. injection of therapeutic αCAR *IGF-1* LV. More specifically, in our initial cohorts, we observed two female mice that survived up to 197 and 198 days, respectively, while in a separate cohort a male mouse survived up to 240 days which account for extension of survival of up to 27% and 54%, respectively. So far we are the first to report such a survival effect. However, when all cohorts tested were combined, mean survival was significantly extended by 14 and 9 days when compared with nontreated and VSVG *IGF-1* LV-treated control cohorts, respectively. Although our sample size was sufficient to detect a medium effect with 80% power, our observations further demonstrate the necessity of including large animal numbers in order to detect meaningful therapeutic effect.[26] Variability reported in our study may be attributed to a number of factors such as: (i) the delivery strategy, as muscle injection cannot by principle be accurate as far as the injection point and depth is concerned, (2) the given dose used, as only 50% of particles injected are expected to be functional,[22] or (3) even the strength of expression of the transgene itself, which is controlled by a CMV enhancer/promoter.

Thus, interpreting and comparing the results of various *IGF-1* ALS studies may be challenging even when the same delivery route is chosen as other factors such as disease variability linked to the animal model or *IGF-1* isoform utilized can contribute to this variability.

Sex-specific differences in disease onset and progression as well as response to therapy have been reported in a number of studies.[17,25,34] In the current study, we found no significant difference when we compared overall disease onset and survival between male and female αCAR *IGF-1* LV-treated mice. No significant difference was also observed in both cases between nontreated and VSVG *IGF-1*- treated control groups. To determine whether neuroprotection can result from retrogradely transported muscle-produced *IGF-1* we included in our study VSVG *IGF-1* LVs injected control cohorts. Interestingly, we observed differences in disease onset between the treatment groups only in male mice (Fig. 2). Disease onset was significantly delayed in male αCAR *IGF-1* LV-treated mice when compared with nontreated male mice, however this was not significant when compared with VSVG *IGF-1*-treated male cohort. Unlike males, in female mice, disease onset was delayed and survival was extended significantly in comparison to both control cohorts. Similar differences in body weight maintenance and motor function were observed between αCAR *IGF-1* LV and VSVG *IGF-1* LV-treated male cohorts (Figs. 2D and 3A). A possible explanation for this could be that MN rescue by αCAR *IGF-1* LV treatment possibly slowed muscle atrophy and consequent weight loss. However, because VSVG *IGF-1* LV-treated male mice also maintained their weights, it is likely that weight was maintained in *IGF-1*-treated mice because *IGF-1* had an anabolic effect on the injected muscles (local expression) and consequently these mice were better able to feed and perform on the rotarod.

It is known that *IGF-1* has a key role both in muscle and nerve tissue anabolism and consequently locally enhances muscle and promotes neuronal survival.[35–37] The *IGF-1* gene, which encodes *IGF-1* undergoes alternative splicing producing multiple isoforms. One of these isoforms, the IGF-1Ea, which is used in this study, is the main supply of anabolic agent in the form of mature *IGF-1*[38,39] and is produced by active muscle.[40] When provided as a muscle-specific transgene it results in muscle hypertrophy and enhances regeneration upon injury.[40–42] Several studies have reported that muscle restricted expression of muscle-specific IGF-1Ea (m*IGF-1*) isoforms in SOD1^{G93A} mice resulted in enhanced MN survival, delayed disease onset, and stabilized the NMJ.[11,43,44] Moreover, localized overexpression of IGF-1Ea has been shown to protect a range of different tissues, including skeletal muscle, against neurodegenerative diseases without increasing systemic *IGF-1* levels.[11,45] In a recent study, Barton and colleagues showed that viral expression of IGF-1Ea and not of mature *IGF-1* promotes the hypertrophic response of muscle in vivo.[46]

Thus, this can explain the effect we observe in VSVG *IGF-1* LV-treated male cohorts both in body weight maintenance and rotarod performance. A CMV enhancer/promoter is active in muscle, and upon intramuscular injection of VSVG *IGF-1* LV, the expression of IGF1-Ea in transduced myofibers can have an anabolic effect on the injected muscles and consequently allow these mice to be better able to feed and have disease progression similar to the αCAR *IGF-1* LV-treated ones.

It could be argued that the effect we see in these animals results from retrogradely transported muscle-produced *IGF-1* having a therapeutic effect in their spinal cord MNs. However, this possibility can be excluded as VSVG *IGF-1* LV injected male mice do maintain their body weight, have rotarod performance, and delayed disease onset similar to age-matched αCAR *IGF-1* LV-treated males but their mean survival is not extended (Figs. 2, S1). Most importantly, MN survival in VSVG *IGF-1* LV-injected animals was poor compared with the enhanced MN survival observed as a result of i.m. pretreatment with αCAR *IGF-1* LV (Fig. 4C). These results strongly implicate that localized expression of *IGF-1* in muscle is beneficial, possibly via a muscle enhancement mechanism but does not prolong survival.

Additionally, lack of therapeutic effect or sex-restricted efficacy was observed in studies where the human IGF-1Ea isoform was overexpressed in muscle[47] or upon intraparenchymal spinal cord delivery[17] in SOD1^{G93A} mice. The male only effect observed in the second study could not be linked to sex-specific differences[17] according to the authors. Results from the present study demonstrate that female αCAR *IGF-1* LV-treated cohorts appeared to respond better as far as disease progression is concerned, maintaining their weights and motor performance when compared with control groups. However, the extension in survival was similar in both male and female αCAR *IGF-1* LV-treated mice. Additionally, MN survival and long-lasting human *IGF-1* expression in the spinal cord were seen in both males and females (Fig. 4), suggesting that the effect was unlikely related to sex-specific differences.

Unlike most of these studies where *IGF-1* is directly delivered to the muscle, our therapeutic strategy resides on retrogradely transported *IGF-1*. Our targeted therapeutic αCAR *IGF-1* LV allows delivery of *IGF-1* specifically in the spinal MNs by targeting the CAR receptor at the NMJ. This way, *IGF-1* can be directly delivered to the spinal cord MNs which express IGF-R,[32] and via secretion possibly establish an autocrine loop, bypassing the risk of reduced bioavailability of injected *IGF-1* by *IGFBP*.[32]

Assessment of αCAR *IGF-1* LV dose escalation and application of treatment at disease onset in this and new rodent models of disease[48] will provide further information as to the extent of the therapeutic efficacy that can be achieved with this targeted therapeutic vector in ALS. Combinatorial gene therapy utilizing multicistronic LV vectors expressing additional factors, such as heat shock proteins[49] or miR-206,[50] could further enhance the potency of this approach. As the aCAR antibody expressed on the LV surface binds both mouse and human receptors[51] testing in iPSC-derived motor neurons from ALS[52] patients could be possible and might enhance translatability.

In summary, our data highlight a novel noninvasive strategy to specifically deliver therapeutics into spinal cord MNs through single distal i.m. injections, and show for the first time that the antibody-targeted therapeutic αCAR *IGF-1* LV vector is beneficial in disease progression and survival in a mouse model of ALS at the given dose. We are the first to report substantial therapeutic efficacy in vivo with αCAR *IGF-1* LV pretreatment where survival was extended up to 50% compared with VSVG *IGF-1* LV and nontreated controls. These data support that αCAR *IGF-1* LV is a promising candidate for early non-invasive neuroprotective gene therapy in ALS.

Acknowledgments

We thank Matthew Pitt (Great Ormond Street Hospital, London) for demonstration and guidance during intercostal injections. We wish to extend our acknowledgements to Rachel James (Imperial College London) for her help and advice at various stages of this study, to Justyna Glegola (MRC Clinical Sciences Centre, Imperial College London) for her valuable help with tissue extraction, Peter Czapski (Central Biomedical Services, Imperial College London) for his help with ear sampling of $SOD1^{G93A}$ mice. Our warmest thanks go to Richard Reynolds (Imperial College London, Centre for Neuroinflammation and Neurodegeneration) for use of the MSD reader and for providing MSD plates for ELISA. We thank our colleagues Jackie de Belleroche and Maria Kinali for critical reading of this manuscript. This work was supported by a Seventh Framework Programme European Research Council Advanced Grant, no: 233147 and a Proof of Concept Grant no: 620253 to N.D.M. supporting I.E. This paper is dedicated to the memory of the Imperial College educated chemist Donald C Cole (1935–2009).

Author Contributions

I.E. designed and performed in vitro and in vivo experiments and wrote the manuscript. I.M., M.D. and A.T. performed experiments. E.E.I. contributed and consulted in behavioral experiments and helped with monitoring of $SOD1^{G93A}$ mice. N.D.M. conceived and designed the study, acquired grant, supervised the work, and wrote the manuscript.

Conflict of Interest

N.D.M. and I.E. are named inventors on a submitted UK patent no: 1308772.1. No other competing financial interests are declared by the authors.

References

1. Bruijn LI, Miller TM, Cleveland DW. Unraveling the mechanisms involved in motor neuron degeneration in ALS. Annu Rev Neurosci 2004;27:723–749.
2. Mulder DW, Kurland LT, Offord KP, Beard CM. Familial adult motor neuron disease: amyotrophic lateral sclerosis. Neurology 1986;36:511–517.
3. Rosen DR. Mutations in Cu/Zn superoxide dismutase gene are associated with familial amyotrophic lateral sclerosis. Nature 1993;364:362.
4. Gurney ME, Pu H, Chiu AY, et al. Motor neuron degeneration in mice that express a human Cu, Zn superoxide dismutase mutation. Science 1994;264:1772–1775.
5. Duan C. Specifying the cellular responses to IGF signals: roles of IGF-binding proteins. J Endocrinol 2002;175:41–54.
6. Sakowski SA, Schuyler AD, Feldman EL. Insulin-like growth factor-I for the treatment of amyotrophic lateral sclerosis. Amyotroph Lateral Scler 2009;10:63–73.
7. Siddle K, Urso B, Niesler CA, et al. Specificity in ligand binding and intracellular signalling by insulin and insulin-like growth factor receptors. Biochem Soc Trans 2001;29 (Pt 4):513–525.
8. Boillee S, Cleveland DW. Gene therapy for ALS delivers. Trends Neurosci 2004;27:235–238.
9. Seeburger JL, Springer JE. Experimental rationale for the therapeutic use of neurotrophins in amyotrophic lateral sclerosis. Exp Neurol 1993;124:64–72.
10. Azzouz M, Ralph GS, Storkebaum E, et al. VEGF delivery with retrogradely transported lentivector prolongs survival in a mouse ALS model. Nature 2004;429:413–417.
11. Dobrowolny G, Giacinti C, Pelosi L, et al. Muscle expression of a local Igf-1 isoform protects motor neurons in an ALS mouse model. J Cell Biol 2005;168:193–199.
12. Kaspar BK, Llado J, Sherkat N, et al. Retrograde viral delivery of IGF-1 prolongs survival in a mouse ALS model. Science 2003;8:839–842.
13. Kaspar BK, Erickson D, Schaffer D, et al. Targeted retrograde gene delivery for neuronal protection. Mol Ther 2002;5:50–56.

14. Dodge JC, Haidet AM, Yang W, et al. Delivery of AAV-IGF-1 to the CNS extends survival in ALS mice through modification of aberrant glial cell activity. Mol Ther 2008;16:1056–1064.
15. Narai H, Nagano I, Ilieva H, et al. Prevention of spinal motor neuron death by insulin-like growth factor-1 associating with the signal transduction systems in SODG93A transgenic mice. J Neurosci Res 2005;15:452–457.
16. Dodge JC, Treleaven CM, Fidler JA, et al. AAV4-mediated expression of IGF-1 and VEGF within cellular components of the ventricular system improves survival outcome in familial ALS mice. Mol Ther 2010;18:2075–2084.
17. Lepore AC, Haenggeli C, Gasmi M, et al. Intraparenchymal spinal cord delivery of adeno-associated virus IGF-1 is protective in the SOD1G93A model of ALS. Brain Res 2007;1185:256–265.
18. Franz CK, Federici T, Yang J, et al. Intraspinal cord delivery of IGF-I mediated by adeno-associated virus 2 is neuroprotective in a rat model of familial ALS. Neurobiol Dis 2009;33:473–481.
19. Borasio GD, Robberecht W, Leigh PN, et al. A placebo-controlled trial of insulin-like growth factor-I in amyotrophic lateral sclerosis. European ALS/IGF-I Study Group. Neurology 1998;51:583–586.
20. Lai EC, Felice KJ, Festoff BW, et al. Effect of recombinant human insulin-like growth factor-I on progression of ALS. A placebo-controlled study. The North America ALS/IGF-I Study Group. Neurology 1997;49:1621–1630.
21. Sorenson EJ, Windbank AJ, Mandrekar JN, et al. Subcutaneous IGF-1 is not beneficial in 2-year ALS trial. Neurology 2008;71:1770–1775.
22. Eleftheriadou I, Trabalza A, Ellison S, et al. Specific retrograde transduction of spinal motor neurons using lentiviral vectors targeted to presynaptic NMJ receptors. Mol Ther 2014;22:1285–1298.
23. Yang L, Bailey L, Baltimore D, Wang P. Targeting lentiviral vectors to specific cell types in vivo. Proc Natl Acad Sci USA 2006;103:11479–11484.
24. Lei Y, Joo KI, Wang P. Engineering fusogenic molecules to achieve targeted transduction of enveloped lentiviral vectors. J Biol Eng 2009;3:8.
25. Heiman-Patterson TD, Deitch JS, Blankenhorn EP, et al. Background and gender effects on survival in the TgN (SOD1-G93A)1Gur mouse model of ALS. J Neurol Sci 2005;236:1–7.
26. Scott S, Kranz JE, Cole J, et al. Design, power, and interpretation of studies in the standard murine model of ALS. Amyotroph Lateral Scler 2008;9:4–15.
27. Alexander GM, Erwin KL, Byers N, et al. Effect of transgene copy number on survival in the G93A SOD1 transgenic mouse model of ALS. Brain Res Mol Brain Res 2004;130:7–15.
28. Martin LJ, Liu Z, Chen K, et al. Motor neuron degeneration in amyotrophic lateral sclerosis mutant superoxide dismutase-1 transgenic mice: mechanisms of mitochondriopathy and cell death. J Comp Neurol 2007;500:20–46.
29. Carpentier DC, Vevis K, Trabalza A, et al. Enhanced pseudotyping efficiency of HIV-1 lentiviral vectors by a rabies/vesicular stomatitis virus chimeric envelope glycoprotein. Gene Ther 2012;19:761–774.
30. Rothstein JD, Dykes-Hoberg M, Pardo CA, et al. Knockout of glutamate transporters reveals a major role for astroglial transport in excitotoxicity and clearance of glutamate. Neuron 1996;16:675–686.
31. Lunetta C, Serafini M, Prelle A, et al. Impaired expression of insulin-like growth factor-1 system in skeletal muscle of amyotrophic lateral sclerosis patients. Muscle Nerve 2012;45:200–208.
32. Wilczak N, de Vos RA, De Keyser J. Free insulin-like growth factor (IGF)-I and IGF binding proteins 2, 5, and 6 in spinal motor neurons in amyotrophic lateral sclerosis. Lancet 2003;361:1007–1011.
33. Dirren E, Aebischer J, Rochat C, et al. SOD1 silencing in motoneurons or glia rescues neuromuscular function in ALS mice. Ann Clin Transl Neurol 2015;2:167–184.
34. Veldink JH, Bar PR, Joosten EA, et al. Sexual differences in onset of disease and response to exercise in a transgenic model of ALS. Neuromuscul Disord 2003;13:737–743.
35. Bodine SC, Stitt TN, Gonzalez M, et al. Akt/mTOR pathway is a crucial regulator of skeletal muscle hypertrophy and can prevent muscle atrophy in vivo. Nat Cell Biol 2001;3:1014–1019.
36. Festoff BW, Yang SX, Vaught J, et al. The insulin-like growth factor signaling system and ALS neurotrophic factor treatment strategies. J Neurol Sci 1995;129 (Suppl):114–121.
37. Lewis ME, Neff NT, Contreras PC, et al. Insulin-like growth factor-I: potential for treatment of motor neuronal disorders. Exp Neurol 1993;124:73–88.
38. Goldspink G, Yang SY. The splicing of the IGF-I gene to yield different muscle growth factors. Adv Genet 2004;52:23–49.
39. Rotwein P. Two insulin-like growth factor I messenger RNAs are expressed in human liver. Proc Natl Acad Sci USA 1986;83:77–81.
40. Musaro A, McCullagh K, Paul A, et al. Localized Igf-1 transgene expression sustains hypertrophy and regeneration in senescent skeletal muscle. Nat Genet 2001;27:195–200.
41. Coleman ME, DeMayo F, Yin KC, et al. Myogenic vector expression of insulin-like growth factor I stimulates muscle cell differentiation and myofiber hypertrophy in transgenic mice. J Biol Chem 1995;270:12109–12116.

42. Rabinovsky ED, Gelir E, Gelir S, et al. Targeted expression of IGF-1 transgene to skeletal muscle accelerates muscle and motor neuron regeneration. FASEB J 2003;17:53–55.
43. Dobrowolny G, Aucello M, Molinaro M, Musaro A. Local expression of mIgf-1 modulates ubiquitin, caspase and CDK5 expression in skeletal muscle of an ALS mouse model. Neurol Res 2008;30:131–136.
44. Palazzolo I, Stack C, Kong L, et al. Overexpression of IGF-1 in muscle attenuates disease in a mouse model of spinal and bulbar muscular atrophy. Neuron 2009;63:316–328.
45. Schertzer JD, van der Poel C, Shavlakadze T, et al. Muscle-specific overexpression of IGF-I improves E-C coupling in skeletal muscle fibers from dystrophic mdx mice. Am J Physiol Cell Physiol 2008;294:C161–C168.
46. Barton ER, DeMeo J, Lei H. The insulin-like growth factor (IGF)-I E-peptides are required for isoform-specific gene expression and muscle hypertrophy after local IGF-I production. J Appl Physiol 2010;108:1069–1076.
47. Messi ML, Clark HM, Prevette DM, et al. The lack of effect of specific overexpression of IGF-1 in the central nervous system or skeletal muscle on pathophysiology in the G93A SOD-1 mouse model of ALS. Exp Neurol 2007;207:52–63.
48. Chew J, Gendron TF, Prudencio M, et al. Neurodegeneration. C9ORF72 repeat expansions in mice cause TDP-43 pathology, neuronal loss, and behavioral deficits. Science 2015;348:1151–1154.
49. Gifondorwa DJ, Robinson MB, Hayes CD, et al. Exogenous delivery of heat shock protein 70 increases lifespan in a mouse model of amyotrophic lateral sclerosis. J Neurosci 2007;27:13173–13180.
50. Williams AH, Valdez G, Moresi V, et al. MicroRNA-206 delays ALS progression and promotes regeneration of neuromuscular synapses in mice. Science 2009;326:1549–1554.
51. Bergelson JM, Cunningham JA, Droguett G, et al. Isolation of a common receptor for Coxsackie B viruses and adenoviruses 2 and 5. Science 1997;275:1320–1323.
52. Kiskinis E, Sandoe J, Williams LA, et al. Pathways disrupted in human ALS motor neurons identified through genetic correction of mutant SOD1. Cell Stem Cell 2014;14:781–795.

Supporting Information

Additional Supporting Information may be found online in the supporting information tab for this article:

Figure S1. Intramuscular delivery of αCAR *IGF-1* LV delayed disease onset and extended survival in both male and female $SOD1^{G93A}$ mice. (A, left panel) In male $SOD1^{G93A}$ mice αCAR *IGF-1* LV treatment significantly delayed median disease onset by 29.5 days when compared with nontreated control mice (145 vs. 115.5 days $P < 0.0001$ Wilcoxon, signed-rank test). No significant delay was observed versus VSVG *IGF-1*-treated mice (6 days). (A, right panel) In the female $SOD1^{G93A}$ mice, treatment with αCAR *IGF-1* significantly delayed median disease onset versus both nontreated and VSVG *IGF-1*-treated control mice by 32.5 days 9 days (153 vs. 120.5, $P < 0.0001$; 153 vs. 144, $P = 0.0087$) , respectively. (B) Median survival of both male and female αCAR *IGF-1* LV-treated mice, was significantly increased versus non-treated control cohorts by 12 and 8 days respectively (males $\chi^2 = 8.513$, $P = 0.0035$; females $\chi^2 = 7.913$, $P = 0.0049$). When compared with VSVG *IGF-1*-treated cohorts, αCAR *IGF-1* LV treatment significantly increased median lifespan of both female (7.5 days $\chi^2 = 4.756$, $P = 0.0292$) and male mice (4 days; $\chi^2 = 4.518$, $P = 0.0335$).

Figure S2. Graphical output of the digital and manual systems for gait analysis. Stride length is the distance in millimetres between successive placements of the same paw. (A) Representative images of footprint analysis produced by the Caltwalk digital system showing the walking pattern of the mouse in the top panel, and a time-based diagram of the paw prints in the bottom panel. Two representative mice (a treated and a nontreated) are presented at two different stages of the disease: presymptomatic stage (70 days old) and late symptomatic stage (135 days old). Prints of paws are marked as RH (right hind; magenta), RF (right front; light blue), LH (left hind; green) and LF (left front; yellow). The length of each bar at the bottom panel indicates the duration of the stance phase of that particular paw, whereas the space between bars indicates the duration of the swing phase. Footprints of late symptomatic stage showed that untreated $SOD1^{G93A}$ mice dragged hind legs whereas αCAR *IGF-1* LV-treated mice showed minor defects in coordination of steps. (B) Representative photos of manual footprint analysis of $SOD1^{G93A}$ mice (treated and nontreated) at late symptomatic stage, showed impaired walking patterns in nontreated control animals compared to aged-matched αCAR *IGF-1* LV-treated mice. Green front paws; red hind paws. Shown is one run representative of five successful runs.

Figure S3. Intrastriatal injections of αCAR *GFP* LV in rats. eGFP expression at the site of injection (striatum) and distal sites (olfactory bulb) injected with αCAR-targeted lentiviral vector. (A) 30 μm thick brain sections from $n = 6$ ($n = 3$ per group) rats harvested at 3 weeks postinjection were obtained and stained with anti-eGFP antibody to enhance the eGFP signal (shown in black). High magnification inserts corresponding to marked regions (dashed box) of the panoramic section images indicate the transduction of cell bodies and fibres. Panoramic section images were captured by epifluorescent

microscope either with a 10× objective (olfactory bulb) or 4× objective (striatum). Colour inserts were captured at site of injection with confocal microscope. Sections were triple stained, using anti-eGFP antibody shown in green, antibody to NeuN shown in red, and antibody to GFAP shown in magenta. (B) Quantification of vector tropism in the striatum. Scale bars, 50 μm.

Table S1. Experimental design

Table S2. Lentiviral preparations for Intrastriatal injections

